The *Plasmodium falciparum* circumsporozoite protein produced in *Lactococcus lactis* is pure and stable

Received for publication, September 27, 2019, and in revised form, November 3, 2019 Published, Papers in Press, December 2, 2019, DOI 10.1074/jbc.RA119.011268

Susheel K. Singh[‡§¶], Jordan Plieskatt[‖], Bishwanath Kumar Chourasia[‡§¶], Vandana Singh[‡§¶], Judith M. Bolscher[**], Koen J. Dechering[**], Bright Adu[‡‡], Blanca López-Méndez[§§], Swarnendu Kaviraj[¶¶], Emily Locke[‖], C. Richter King[‖], and Michael Theisen[‡§¶1]

From the [‡]Department for Congenital Disorders, Statens Serum Institut, 2300 Copenhagen, Denmark, the [§]Centre for Medical Parasitology at Department of Immunology and Microbiology and [§§]Novo Nordisk Foundation Center for Protein Research, Faculty of Health and Medical Sciences, University of Copenhagen, 2200 Copenhagen, Denmark, the [¶]Department of Infectious Diseases, Copenhagen University Hospital, Rigshospitalet, 2100 Copenhagen, Denmark, [‖]PATH's Malaria Vaccine Initiative, Washington, D. C. 20001, [**]TropIQ Health Sciences, 6534 AT Nijmegen, The Netherlands, the [‡‡]Noguchi Memorial Institute for Medical Research, University of Ghana, Legon, Ghana, and [¶¶]Gennova Biopharmaceuticals Limited, Pune 411057, India

Edited by Peter Cresswell

The *Plasmodium falciparum* circumsporozoite protein (PfCSP) is a sporozoite surface protein whose role in sporozoite motility and cell invasion has made it the leading candidate for a pre-erythrocytic malaria vaccine. However, production of high yields of soluble recombinant PfCSP, including its extensive NANP and NVDP repeats, has proven problematic. Here, we report on the development and characterization of a secreted, soluble, and stable full-length PfCSP (containing 4 NVDP and 38 NANP repeats) produced in the *Lactococcus lactis* expression system. The recombinant full-length PfCSP, denoted PfCSP4/38, was produced initially with a histidine tag and purified by a simple two-step procedure. Importantly, the recombinant PfCSP4/38 retained a conformational epitope for antibodies as confirmed by both *in vivo* and *in vitro* characterizations. We characterized this complex protein by HPLC, light scattering, MS analysis, differential scanning fluorimetry, CD, SDS-PAGE, and immunoblotting with conformation-dependent and -independent mAbs, which confirmed it to be both pure and soluble. Moreover, we found that the recombinant protein is stable at both frozen and elevated-temperature storage conditions. When we used *L. lactis*–derived PfCSP4/38 to immunize mice, it elicited high levels of functional antibodies that had the capacity to modify sporozoite motility *in vitro*. We concluded that the reported yield, purity, results of biophysical analyses, and stability of PfCSP4/38 warrant further consideration of using the *L. lactis* system for the production of circumsporozoite proteins for preclinical and clinical applications in malaria vaccine development.

Malaria is a vector-borne disease caused by parasites of the *Plasmodium* genus with *Plasmodium falciparum* responsible for an estimated 219 million cases of malaria and 435,000 deaths worldwide (1). Of 91 countries reporting indigenous malaria cases in 2016, 15 countries—all in sub-Saharan Africa, except India— carried 80% of the burden (1). Although artemisinin combination therapy, intermittent preventive treatment of pregnant women and children, and enhanced vector control contribute to malaria control, new tools are needed, including vaccines, to contain and eventually eradicate malaria (2).

The *P. falciparum* circumsporozoite protein (PfCSP) covers the surface of the sporozoite and is critical to sporozoite development in the mosquito and cell invasion in the mammalian host (3–5). PfCSP is the leading pre-erythrocytic vaccine candidate and the basis for the most advanced malaria vaccine, RTS,S (Mosquirix®). RTS,S contains the central and C-terminal domains of PfCSP genetically fused to the hepatitis B virus surface antigen (6). RTS,S has completed phase 3 clinical trials and is found to prevent ~39% of malaria cases and 29% cases of severe malaria in infants or children during 12 months of follow-up (7, 8). The vaccine is considered safe, but because the efficacy was rather short-lived, there is a need to generate a second generation, more efficacious vaccine (9). Because RTS,S only contains the central repeat region and C-terminal domains of PfCSP, including only 19 of the 38 NANP repeats, it has been of interest to explore protein constructs representing the full-length sequence, including the full 38 NANP and 4 NVDP repeat motifs. Despite many efforts, the full-length and full-repeat ~42-kDa PfCSP has proven to be a difficult target for production in most heterologous expression systems (6, 10–14), possibly because of the difficulties in the formation of correctly folded protein. Such difficulty, including low-expression or aggregation of full-length CSP molecules beyond RTS,S, has often led to a shortened construct selected for manufacture (12).

Proper folding of cysteine-containing proteins such as PfCSP, which includes two disulfide pairs and a fifth N-terminal cysteine, depends on the correct formation of disulfide bonds. Accordingly, we have used the Gram-positive *Lactococcus lactis*, a well-established host for heterologous expression of disulfide-bonded proteins (15–17), for the production of a recom-

This work was funded by PATH's Malaria Vaccine Initiative under Grant OPP1108403 from the Bill & Melinda Gates Foundation and in part by Grant NNF14CC0001 from the Novo Nordisk Foundation Center for Protein Research. The authors declare that they have no conflicts of interest with the contents of this article.

This article contains Figs. S1–S3.

[1] To whom correspondence should be addressed: Dept. for Congenital Disorders, Statens Serum Institut, Artillerivej 5, 2300 Copenhagen, Denmark. Tel.: 45-20888302; E-mail: mth@ssi.dk.

binant PfCSP containing 4 cysteines and the full 38 NANP and 4 NVDP repeats.

PfCSP can be divided into three regions: the N-terminal region containing a highly conserved KLKQP motif (termed region I), which binds heparin sulfate proteoglycans, the central repeat region containing the NANP and NVDP protein motifs, and the C-terminal region containing the thrombospondin-like type I repeat (TSR)[2] (18). Whereas the central repeat region varies in length among *P. falciparum* isolates, the amino acid sequence of the repeat motif is conserved, suggesting that they are structurally or functionally important, although not proven (18), and elicit strong immune responses (19, 20). Irrespective of their biological roles, each of the individual regions provides an opportunity as a vaccine target, which supports the rationale to explore a recombinant PfCSP antigen as a vaccine candidate that encompasses as much of the native protein sequence as possible, including the full number of NANP and NVDP repeats. The N-terminal region contains an epitope that interacts with liver cells through heparin sulfate (21). Antibodies against this epitope are highly inhibitory in a sporozoite invasion assay (21). The junction between the N-terminal and central repeat regions contains an epitope targeted by potent neutralizing antibodies (22, 23), one of which provides sterile protection in mice (23). The central repeat region is a major target for antibodies functional in i*n vitro* and *in vivo* assays (24, 25), and the C-terminal region contains B-cell epitopes and one or more $CD8^+$ T-cell epitopes (26, 27).

To advance development of PfCSP for both preclinical and clinical work, we developed a scalable production process for a recombinant PfCSP containing 4 cysteines and 38 NANP and 4 NVDP repeats encompassing amino acids 26–383 of the native molecule. Knowing from prior reports that aggregation, solubility, and proper conformation may be of concern for CSP-based recombinant proteins, we interrogated the purified protein by a variety of biochemical and biophysical methods to profile its purity, structure, and stability. Here, we found PfCSP4/38 to be pure, soluble, and predominantly monomeric. Based on characterization with conformational mAbs, we found the recombinant protein to contain proper epitopes. When evaluated with biophysical tools such as CD or differential scanning fluorimetry (DSF), the protein was shown to be of proper secondary structure and thermally stable.

To compliment the biophysical and biochemical characterization of PfCSP4/38 and determine whether the recombinant PfCSP4/38 could elicit antibodies similar to the native molecule, the protein was tested for functional immunogenicity in mice using two adjuvants including the human-acceptable Alhydrogel®. The specificity of induced antibodies was then assessed by ELISA and their capacity for inhibition of sporozoite motility in the 1) gliding motility assay, 2) sporozoite traversal inhibition assay, and 3) hepatocyte invasion inhibition assay.

[2] The abbreviations used are: TSR, thrombospondin-like type I repeat; DSF, differential scanning fluorimetry; CSP, circumsporozoite protein; IEC, ion-exchange chromatography; MALS, multiangle light scattering; SEC, size-exclusion chromatography; DLS, dynamic light scattering; RP, reversed-phase; HRP, horseradish peroxidase; SE, size exclusion.

It should be noted that other CSP-based molecules in clinical evaluation such as R21 (28) continue to utilize shortened repeat motifs (similar to RTS,S) or employ specialized expression platforms such as *Pseudomonas fluorescens* (11). Here, we report on the comprehensive characterization of a recombinant CSP molecule containing the full 4 NVDP and 38 NANP repeats, which may further serve as a reference protein or vaccine immunogen. This information, taken together, continues to support *L. lactis* as a suitable expression system for disulfide-dependent complex malaria antigens and provides a basis for further development of PfCSP recombinant proteins in the system for which a pure and stable protein is required.

Results

Expression and purification of a secreted and soluble PfCSP4/38

The construct design of full-length PfCSP (amino acids 26–383) was based on prior designs (12) that omit the fifth (unpaired) N-terminal cysteine and encompasses the full repeat region along with the four C-terminal cysteines. The PfCSP gene based on the native molecule *P. falciparum* 3D7 and containing a C-terminal six-histidine tag to aid initial expression and characterization studies was then codon-optimized and cloned into the *L. lactis* expression system (Fig. 1*A*). The secreted protein was purified from the culture supernatant by sequential immobilized metal affinity chromatography and ion-exchange chromatography (IEC) with a final yield of ~25 mg/liter. The recombinant PfCSP protein was found to be more than 95% pure, with SDS-PAGE showing a major band of 60 kDa corresponding to monomeric PfCSP4/38 (Fig. 1*B*). Immune blotting with an anti-His antibody revealed a predominant band corresponding to the monomeric form and a minor band corresponding to a multimeric form (Fig. 1*C*). Immune blotting with a polyclonal antibody raised against *L. lactis* culture supernatant proteins revealed a minor band corresponding to contaminating host cell protein (Fig. 1*D*, *lane 3*). Lastly, to demonstrate consistency and scalability, the production process was successfully scaled from 1-liter to 5-liter and resulted in a similarly pure and stable molecule (Table 1).

Protein characterization of recombinant PfCSP4/38 indicates a properly folded, pure, and stable molecule

Because protein folding is essential for the presentation of antibody epitopes, PfCSP4/38 was examined by Western blotting analysis with mAb1A6 and mAb1E8 directed against conformational and linear epitopes in the C terminus, respectively (Fig. 2*A*). As expected, mAb1A6 reacted strongly with the folded protein (nonreduced) and only weakly with the reduced unfolded form of PfCSP4/38 (Fig. 2*A*). In contrast, mAb1E8 reacted strongly with reduced PfCSP4/38 and weakly with nonreduced PfCSP4/38, suggesting that the linear epitope remains buried within the folded protein sequence (Fig. 2*A*).

Disulfide bond formation was confirmed by demonstrating very low levels of free thiol groups (<1%) under native conditions (data not shown). The molecular mass of nonreduced PfCSP4/38 as determined by LC-MS was 39624.8 Da (Fig. 2*B*). This molecular mass corresponds well to the predicted mass of 39623.8 Da, assuming that PfCSP4/38 contains the vector-en-

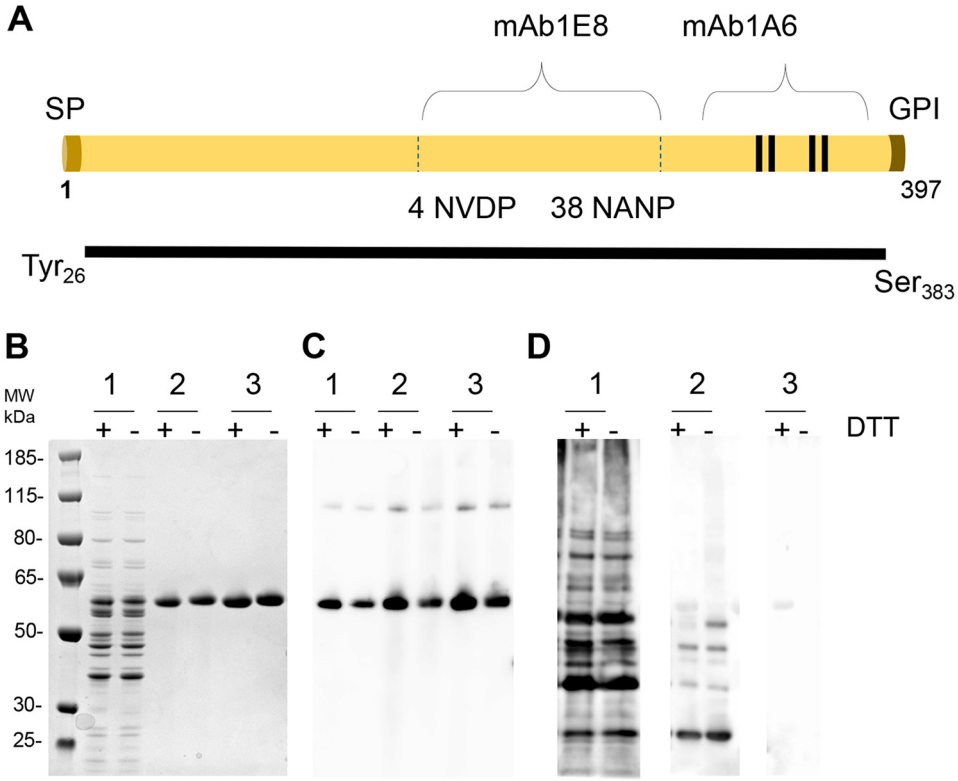

Figure 1. Production of PfCSP4/38 in *L. lactis*. *A*, schematic representation of PfCSP4/38 containing the full repeat region (4 NVDP/38NANP), which is reactive to mAb 1E8. The positions of the signal peptide (*SP*), the central repeat region containing the NVDP and NANP protein units, and the glycosylphosphatidylinositol (*GPI*) anchor are indicated. The four C-terminal cysteines are indicated with *lines* and are reactive to the conformational mAb 1A6. The N terminus along with the N-terminal cysteine are omitted, with sequence originating at Tyr-26 and terminating prior to GPI anchor of C terminus (Ser-383). Recombinant PfCSP4/38 protein contains the vector-encoded amino acid residues AERS at the N-terminal end and a short flexible linker (GGS) followed by a six-histidine tag at the C-terminal end. *B*, Coomassie Blue–stained 4–12.5% polyacrylamide gel of 1) fermentation supernatant, 2) immobilized metal affinity chromatography–purified PfCSP protein elution, and 3) IEC-purified PfCSP protein elution. *C* and *D*, an immune blot analysis of the same gel shown in *B* with anti-His (*C*) and anti–*L. lactis* antibody (*D*). PfCSP4/38 at 1 and 0.5 μg was loaded on gels, Coomassie-stained, or transferred for Western blots, respectively, under reducing (+) or nonreducing (−) conditions with 10 mM DTT. The sizes (kDa) of the molecular mass (*MW*) markers are indicated.

Table 1

Biochemical characteristics of recombinant PfCSP4/38 produced from *L. lactis*

Shown are the results obtained for recombinant PfCSP4/38 produced at both the 1- and 5-liter scale. Nonreducing (NR) and reducing (R) conditions are noted where tested.

Test	Method	Specification	Result	
			1 liters	5 liters
pH	pH meter	Report (target 6–8)	7.0	7.0
Color and appearance	Visual observation	Clear, colorless solution free of particles	Clear, colorless solution free of particles	Clear, colorless solution free of particles
Endotoxin	LAL (Limulus amebocyte lysate)	≤100 EU/mg	8 EU/mg	17 EU/mg
Protein content	BCA	>0.4 mg/ml	0.5 mg/ml	0.73 mg/ml
	A_{280}	>0.4 mg/ml	0.5 mg/ml	0.9 mg/ml
Identity and integrity	SDS-PAGE (NR/R)	Predominant band at expected molecular weight ≥85%	Major monomer band	Major monomer band
	Western blot against mAb1A6, mAb1E8, and anti-histidine (NR/R)	Positive identification and predominant band at expected molecular weight	Major monomer band	Major monomer band
Identity, integrity, and purity	SE-HPLC	≥85% monomer	96% monomer	90% monomer
	RP-HPLC	>85%	94.9%	93%
Molecular mass	Intact mass spectroscopy via LC-MS/MS (NR/R)	Main peak ± 10 Da of expected mass	NR: 39624.8173 Da	NR: 39624.8161 Da
		NR: 39,623 Da, R: 39,627 Da	R: 39628.8527 Da	R: 39628.8532 Da

coded amino acid residues AERS at the N-terminal end and a short flexible linker (GGS) followed by a six-histidine tag at the C-terminal end. These results indicate that PfCSP4/38 contains no post-translational modifications and that the secreted, soluble protein was intact. The reduction of PfCSP4/38 resulted in an increase of 4 daltons for a mass of 39,628.8 Da, which is consistent with the presence of two disulfide bonds (Fig. 2*B*). CSP is known to be partially unstructured with a large hydrodynamic radius (14). To determine the absolute molecular mass of PfCSP4/38 without relying on calibration of the size-exclusion chromatography (SEC) column with reference protein standards, we used multiangle light scattering (MALS) coupled with SEC. PfCSP4/38 eluted as a main monodisperse peak at 12.8 ml (Fig. 2*C*) with an average molecular mass of 40.2 kDa, indicating that PfCSP4/38 is a monomer in solution. On-line QELS (quasi-elastic light scattering) measurements shows a hydrodynamic

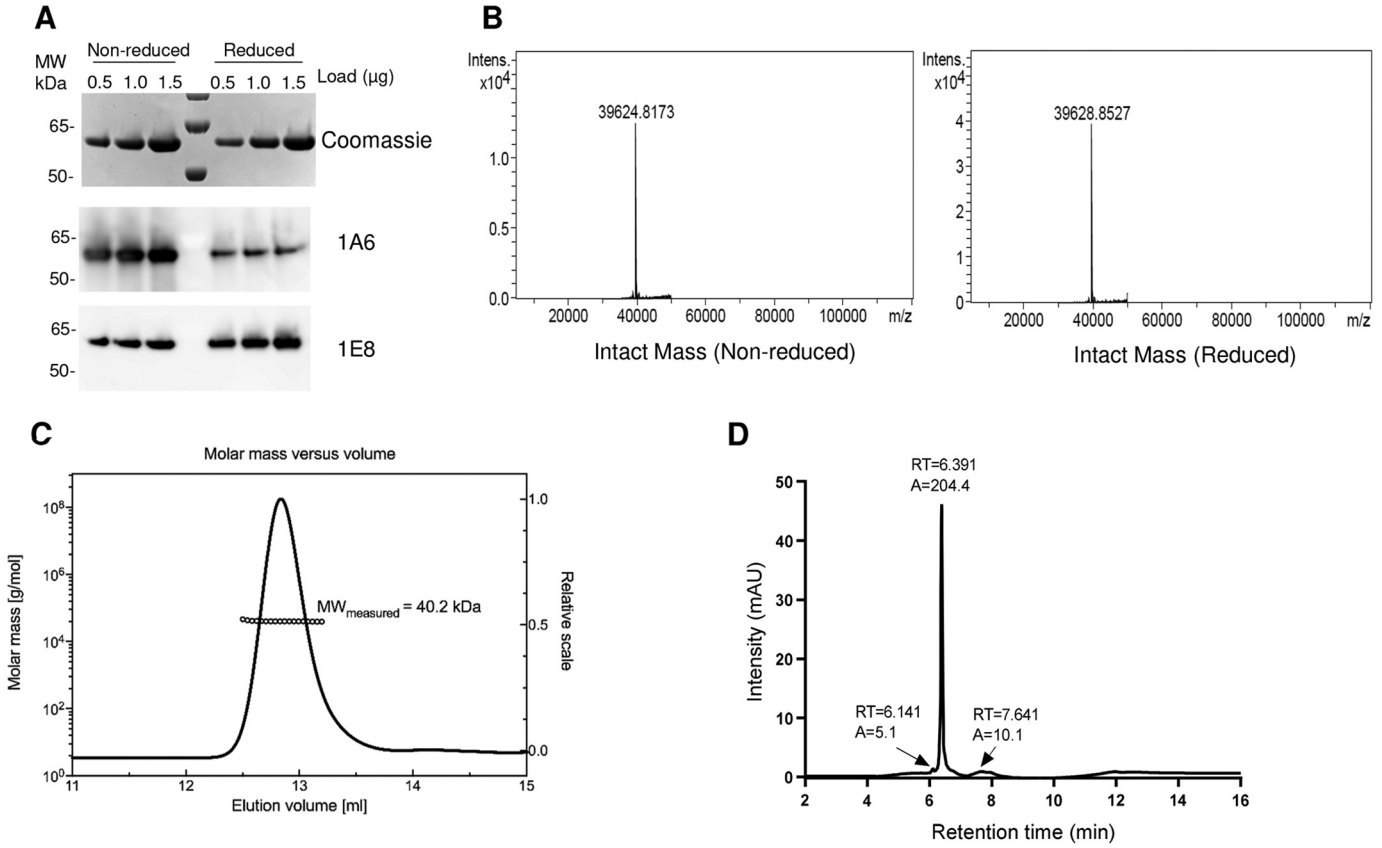

Figure 2. Characterization of PfCSP4/38. *A*, *top panel*, Coomassie Blue–stained 4–12.5% polyacrylamide gel with different amounts (0.5, 1.0, and 1.5 μg of PfCSP) in nonreduced and reduced conditions. *Middle* and *bottom panels*, Western blotting using the same gel loading as in the *top panel* with conformational (mAb 1A6, *middle panel*) and nonconformational (mAb 1E8, *bottom panel*) antibody. The sizes (kDa) of the molecular mass (*MW*) markers are indicated. *B*, deconvoluted mass spectra corresponding to the nonreduced and the reduced samples. *C*, SEC-MALS analysis. PfCSP4/38 was injected onto a Superdex 200 Increase 10/300 GL column, and the change in refractive index as a function of protein concentration was used to compute the molar masses. The *solid line* plotted on the *right axis* corresponds to the chromatogram of the change in refractive index from the SEC column. The *right axis scale* is normalized to the greatest magnitude across the chromatogram data, *i.e.* to the monomer peak of PfCSP4/38. The molar masses across the eluting peak are plotted as *open circles* (for clarity, only every tenth measurement) on the *left axis* (molar mass). The average molecular mass is indicated. *D*, reversed-phase HPLC-UV chromatograms recorded following analysis of purified protein PfCSP. The peak at 6.391 min corresponds to monomeric PfCSP4/38 antigen. In HPLC chromatograms (*D*), *A* denotes integrated peak area, and *RT* indicates retention time.

radius (R_h) at the apex of the peak of ≈4.3 nm in agreement with an extended structure compared with globular proteins of similar molar mass that elute at later retention times (Fig. S1).

The purity of the final PfCSP4/38 protein samples was also assessed by reversed-phase HPLC. There PfCSP4/38 eluted as a main peak at 6.39 min (Fig. 2*D*). The presence of few minor peaks indicates a homogenous population of PfCSP4/38 protein species with a relative purity of 94.9% (Fig. 2*D*).

Biophysical characterization of PfCSP4/38

Prior biophysical characterization of recombinant CSP has either been limited or limited to recombinant proteins including only shortened repeat regions; therefore we wished both to further evaluate the secondary structure of the recombinant protein reported here and to demonstrate thermal stability. PfCSP4/38 consists of a homogenous population of mainly monomeric protein species, both pre- and post-thermal elevation, as demonstrated by dynamic light scattering (DLS) and static light scattering experiments (Fig. 3*A*). The secondary structure of PfCSP4/38 at 20 °C was analyzed by CD (Fig. 3*B*). The deconvolution of the far-UV spectra using the Dichroweb server (29) and the CDSSTR algorithm (30) shows a content of secondary structure of 5% (±1) α-helix, 22% (±9) β-sheet, 16% (±8) β-turn, and 57% (±8) random coil in agreement with previous studies (14). A cycle of heating to 90 °C and cooling to 20 °C gives very similar CD spectra, indicating reversible thermal denaturation. The stability of the tertiary structure of PfCSP4/38 was monitored through differential scanning fluorimetry (nanoDSF), and the thermal stability measurements showed only the onset of a single thermal transition above 80 °C (Fig. 3*C*). These results, taken together, indicate that the conformation and structure of monomeric PfCSP4/38 was highly stable, even at elevated temperatures.

Lastly, the stability of PfCSP4/38 was assessed for five cycles of freeze/thaw and in an accelerated stability study at 4 or 37 °C for up to 30 days (Fig. S2). Samples taken at 0, 1, 2, 7, 15, and 30 days were analyzed on the same day by SDS-PAGE and immune blotting with mAb1A6 against the conformational epitope of PfCSP and anti-His antibody. Banding patterns remained unchanged at both temperatures, further indicating the thermal stability of PfCSP4/38. It should also be noted that PfCSP4/38 remained in solution during the stability studies with PfCSP4/38, remaining a clear colorless solution free of particulates.

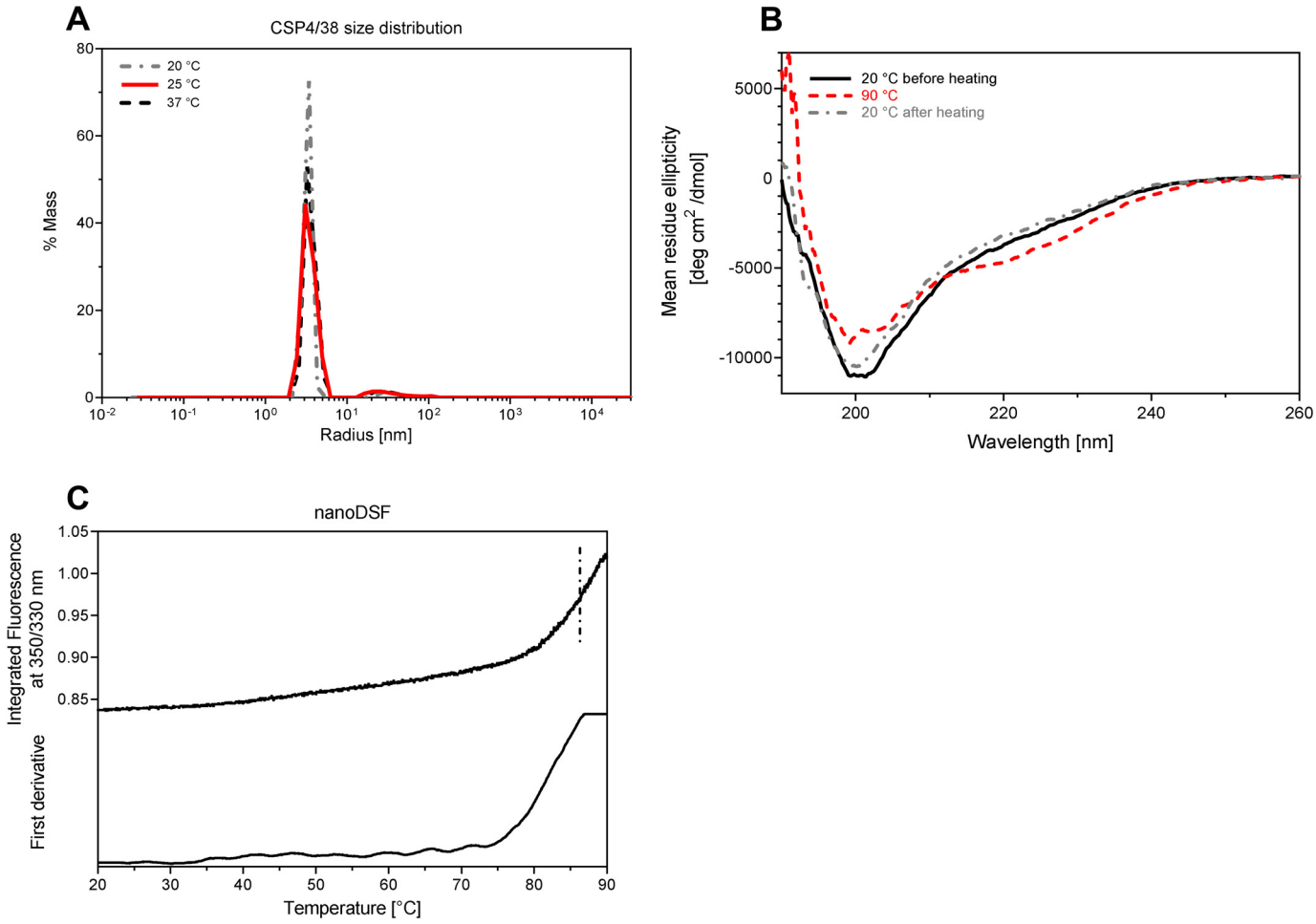

Figure 3. Biophysical studies of PfCSP4/38. *A*, distributions of hydrodynamic radii obtained from DLS on PfCSP4/38 at three different temperatures. *B*, CD spectra of PfCSP4/38 measured at two different temperatures: 20 and 90 °C (*red dashed line*). CD spectra were recorded at 20 °C before (*dark solid line*) and after (*gray dashed line*) heating the protein sample at 90 °C. Mean residue ellipticity (deg cm^2 $dmol^{-1}$) is plotted as a function of the wavelength (nm). *C*, differential scanning fluorimetry (nano-DSF) spectra of PfCSP4/38. Fluorescence intensities at single wavelengths of 350 nm (F_{350}) and 330 nm (F_{330}) were recorded. The F_{350}/F_{330} ratio (*upper panel*) and its first derivative (*lower panel*) are plotted as functions-of the temperature.

Antigenicity of recombinant PfCSP4/38

The antigenicity of PfCSP4/38 was evaluated by ELISA against plasma samples from adults living in an area of Liberia where malaria is holoendemic. Plasma samples from Danish donors never exposed to malaria were used as controls. PfCSP4/38 reacted in the IgG ELISA with 82 (97%) of the 84 plasma samples from Liberia (Fig. 4). The same samples were also assessed for antibodies against the asexual blood stage GLURP-R2 (31, 32), as a control antigen, confirming that the plasma samples contain high levels of malarial IgG antibodies.

Immunogenicity of recombinant PfCSP4/38

Humoral responses against B-cell epitopes on PfCSP4/38 were determined in mice. A group of CD1 mice ($n = 8$) was immunized three times at 3-week intervals with PfCSP4/38 formulated with Alhydrogel®. Sera collected on days 21, 42, and 56 were tested by ELISA for IgG antibody reactivity against PfCSP4/38. Two injections of PfCSP4/38 elicited high levels of specific antibodies against the immunogen (Fig. S3). Serially diluted pooled terminal mouse sera reacted with native sporozoites in a dose-dependent manner via ELISA (data not shown), demonstrating that the recombinant protein provides an adequate presentation of native PfCSP epitopes. From the sporozoite ELISA, the concentration of elicited PfCSP-specific antibodies in pooled sera was estimated to be 72.4 μg/ml by a

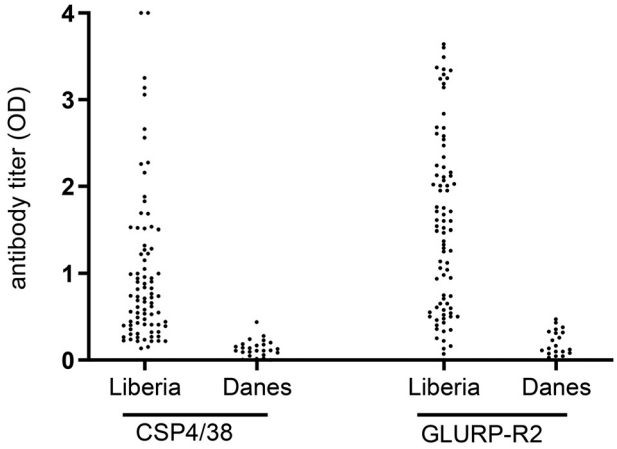

Figure 4. Antigenic analysis of recombinant PfCSP4/38 produced from *L. lactis*. Total IgG prevalence as observed in plasma from 84 Liberian adults and 24 Danish blood donors never exposed to malaria against purified recombinant PfCSP4/38 and GLURP-R2 proteins was determined through ELISA. Antibody titers are expressed as EC_{50} values.

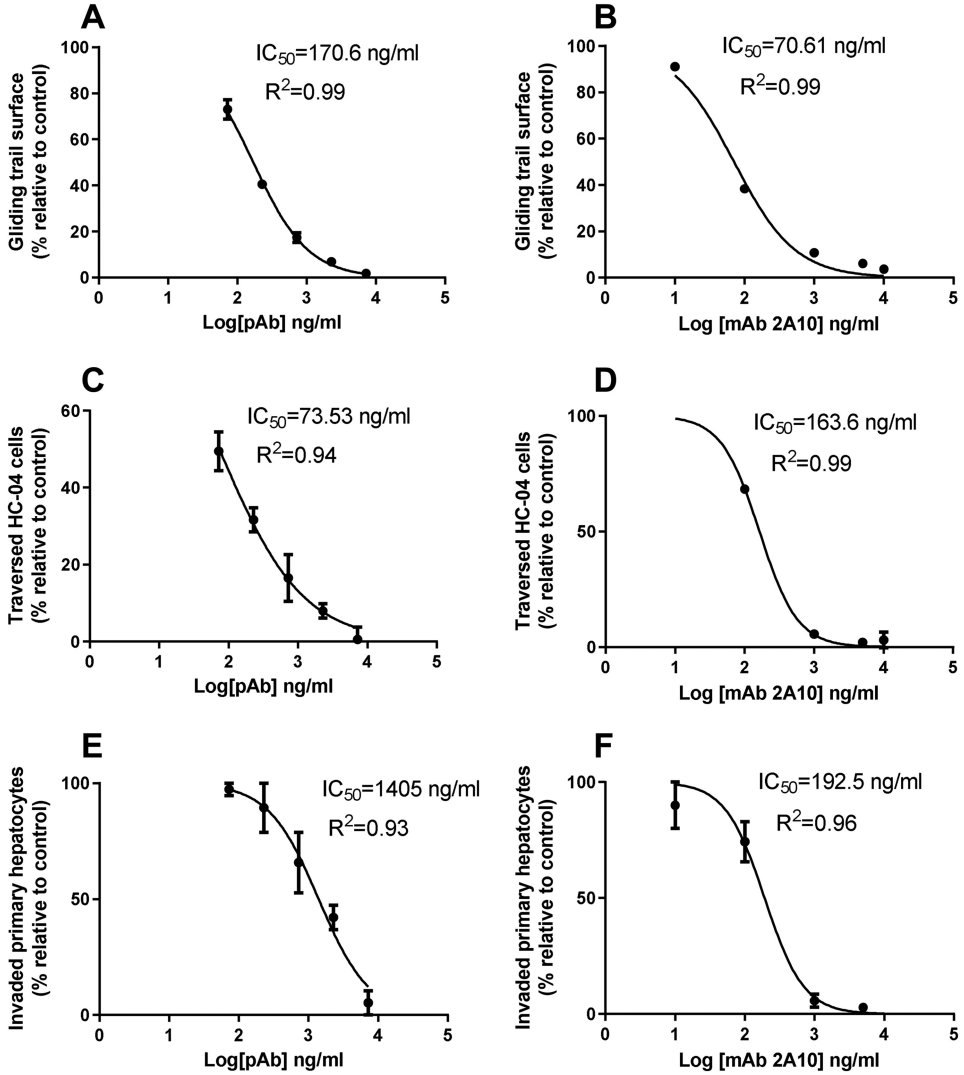

Figure 5. Anti-PfCSP4/38 antibodies inhibit sporozoite gliding motility (*A* and *B*), traversal (*C* and *D*), and liver cell invasion (*E* and *F*). Mouse polyclonal sera containing PfCSP4/38-specific antibodies (*A*, *C*, and *E*) or mAb 2A10 (*B*, *D*, and *F*) were normalized against naïve mouse sera. The initial concentration of mouse polyclonal (PfCSP4/38) IgG in the sera was first determined by sporozoite ELISA where a standard reference curve generated with the mAb2A10 was used to convert the sera-specific optical density values to concentration values using a four-parameter curve fitting program. The assay-specific IC_{50} concentration values were estimated using serial dilutions of the sera based on the determined initial concentration of the polyclonal PfCSP4/38 antibody present. The mAb 2A10 concentrations are from purified IgG. The IC_{50} was calculated by logistic regression using a four-parameter model and least-square method to determine the best fit. The lowest value of each *y* value was set to 0, and the maximum value was set to 100%. *pAb*, polyclonal antibody.

four-parameter logistic curve fit program (31) using a protein reference standard based on a purified IgG antibody (mAb2A10) against the central repeat region of PfCSP (33). In addition, a parallel second study tested the immunogenicity of PfCSP4/38 in a similar mouse model but with two immunizations 28 days apart and utilizing the Montanide ISA720VG adjuvant (Fig. S3). Sera collected at a terminal bleed on day 42 also demonstrated positive reactivity by ELISA (Fig. S3). Given a sufficient immune response was seen with the human-compatible Alhydrogel® adjuvant, the terminal sera from that study were further evaluated via *in vitro* functional assays.

Mouse anti-PfCSP4/38 antibodies inhibit sporozoite motility and invasion of liver cells

Antibodies against PfCSP are known to interfere with sporozoite motility *in vitro* and to block hepatocyte invasion *in vivo* (34). Therefore, the functional activity of mouse anti-PfCSP4/38 antibodies was assessed in different bioassays that monitor parasite motility and cell invasion. In these analyses, the mouse polyclonal sera containing PfCSP4/38 antibodies were assessed alongside the mAb mAb2A10 (33), which was used as a positive control. First, anti-PfCSP4/38 antibodies were tested in the gliding motility assay that is based on the detection of trails of native PfCSP, which are deposited on the surface of microscopic coverslips by the moving sporozoite (35). The number of gliding trails relative to a negative control sample decreased with increasing concentration of anti-PfCSP4/38 antibodies (Fig. 5*A*). The concentration of anti-PfCSP4/38 IgG (170.6 ng/ml in the polyclonal antisera) required to achieve a 50% reduction in gliding motility was ~2.5 times higher than that required for the purified antibody mAb2A10 (70.6 ng/ml) for the same inhibition (Fig. 5*B*).

Next, we examined the functional activity of anti-PfCSP4/38 antibodies in the sporozoite traversal inhibition assay (35). Sporozoites depend on traversal motility to cross the sinusoidal cell layer and multiple liver cells before invasion of the terminal hepatocyte (36). A lower (73.5 ng/ml) amount of mouse anti-PfCSP4/38 antibodies was required for 50% inhibition of sporozoite traversal of HC-04 cells compared with the concentration of the mAb2A10 (163.6 ng/ml) required to achieve same (Fig. 5, *C* and *D*). Finally, anti-PfCSP4/38 antibodies inhibited the invasion of primary hepatocytes in a dose-dependent manner, although the concentration required for 50% invasion inhibition was approximately seven times higher than for the mAb2A10 (Fig. 5, *D* and *E*). The reported assay-specific IC_{50} concentration values were obtained by serial dilution of the sera based on the predetermined concentration of polyclonal PfCSP4/38 antibodies estimated to be present when the sporozoite ELISA was performed. Specifically, the concentration of antibody in each serial dilution was log transformed, and the IC_{50} values were calculated in GraphPad Prism version 6 using the log(inhibitor) *versus* normalized response-variable slope function (GraphPad Prism version 5.00 for Windows; GraphPad Software, San Diego, CA). Collectively, these results demonstrate that the *L. lactis*-produced PfCSP4/38 elicits functional antibodies with the capacity to modify sporozoite motility and invasion of hepatocytes.

Discussion

This study follows several prior attempts to produce full-length PfCSP in a variety of expression systems including *Escherichia coli* (10, 14, 37), baculovirus (Sf9) cells (13), *P. fluorescens* (11), and *Pichia pastoris* (14). Although some of these systems have been suitable for the production of complex malaria antigens, the reported yields and stability of full-length soluble recombinant PfCSP have been generally low (12). This has shifted the focus to the pursuit of shorter or modified PfCSP sequences (12). Additionally, the relatively low yields may be attributed to improper folding caused by nonnative cysteine connectivity. In eukaryotes, misfolded protein may become degraded and ultimately removed through the ubiquitin pathway. In Gram-negative *E. coli*, the recombinant protein is initially produced in the cytoplasm whereas disulfide bonds are formed in the periplasmic space, thus providing a possible explanation for the low yields of disulfide-bonded protein. Indeed, newly developed *E. coli* strains may overcome this limitation (12) and should continue to be explored. Because proper disulfide bond formation is critical not only for high yields of the recombinant protein but also for functional antibody responses (17), we utilized the *L. lactis* expression system to produce PfCSP, which has a proven track record for the secretion of complex malaria antigens (15, 17).

In our effort to produce a full-length PfCSP, a simple workflow was developed consisting of batch fermentation in a lab-scale stirred bioreactor followed by a simple two-step purification process. Because proper folding of PfCSP depends on the formation of two disulfide bonds in the C-terminal TSR domain, we used the activity of the disulfide reduction sensitive and conformational mAb1A6 to monitor the expression and purification of properly folded protein species. The results presented here from immune blotting analysis demonstrate that purified PfCSP4/38 produced in *L. lactis* was strongly recognized by mAb1A6 and thus retained the conformational epitope in the TSR domain. This finding was corroborated by the finding that mAb1E8 against a linear epitope displayed the opposite activity by reacting stronger with reduced compared with nonreduced PfCSP4/38. The characterization by SE-HPLC demonstrates that PfCSP4/38 mainly contains monomers with all four cysteine residues in the oxidized state as shown by MS analysis. Although the cysteine connectivity has not been determined in *L. lactis*-produced PfCSP4/38, as of yet, the immune blotting studies presented here agree well with disulfide bonding being critical for the folding of PfCSP (38).

Further, the final PfCSP4/38 purified yield of 25 mg/liter from the initial process reported here serves as a basis for further process optimization and yields a relatively pure protein of ~95% as reported by RP-HPLC. Immune blotting analysis with a host cell protein-specific polyclonal antiserum suggests that remaining impurities are likely product-related consisting of misfolded protein species and/or degradation products, with little to no reactivity of host-derived products. Aggregation or insolubility has been a concern with recombinant CSP, and therefore it was important to fully characterize the state of PfCSP4/38 in solution by a variety of biochemical and biophysical methods. Accordingly, PfCSP4/38 proved stable for 30 days at 37 °C as determined in the accelerated stability program. In agreement with published data (14), detailed biophysical studies including DLS, SEC-MALS, and CD experiments demonstrated that soluble PfCSP4/38 forms a homogenous population with mainly a monomeric protein species with a predominance of β-sheets and random coil conformations. Further, these analyses showed little shift in the secondary or tertiary structure as a function of temperature, indicating that PfCSP4/38 is thermally stable. Taken together, these results demonstrate that the *L. lactis* system is a promising expression system for PfCSP for further production optimization and development of nontagged variants.

Having shown that PfCSP4/38 maintained the conformational integrity of immunologically relevant regions, we next investigated its antigenicity using serum samples from Liberian adults clinically immune against malaria (39). Almost all (97%) serum samples reacted to PfCSP4/38 via ELISA, demonstrating that PfCSP4/38 provides an adequate presentation of epitopes for naturally acquired human antibodies.

Because the vaccine potential of PfCSP is well-established, it was of interest to investigate the immunogenicity of *L. lactis*-produced PfCSP4/38 in mice. Two injections of PfCSP4/38 elicited high levels of specific antibodies, regardless of the adjuvant, which reacted with native antigens in the sporozoite ELISA. There is strong evidence that anti-CSP antibodies interfere with gliding motility (35). Here we found that mouse anti-PfCSP4/38 antisera strongly inhibited sporozoite motility *in vitro*, suggesting that *L. lactis*-produced PfCSP4/38 provides an adequate presentation of epitopes for functional antibodies. Given that pooled anti-PfCSP4/38 antiserum inhibited sporozoite gliding motility *in vitro*, we next examined the functional activity of mouse antibodies against *L. lactis*-produced PfCSP4/38 in the sporozoite traversal and hepatocyte invasion

assays. In agreement with previous findings (40–42), the anti-PfCSP4/38 antiserum generated here strongly inhibited traversal and invasion. However, the exact epitopes recognized by these functional antibodies remains to be investigated, and no direct comparisons of *L. lactis*-derived PfCSP4/38 with other reported recombinant circumsporozoite proteins (11, 12) were made here.

In conclusion, *L. lactis* proved highly suited for the production of recombinant PfCSP, expressing a soluble secreted protein with apparent proper disulfide formation. A simple manufacturing process for PfCSP4/38 was developed here and provides the basis for further development, including nontagged variants. The resulting stable antigen, predominantly of monomeric state, was frequently recognized by sera from humans clinically immune to malaria. We further demonstrated that PfCSP4/38 elicited high levels of parasite-specific antibodies in mice and that these antibodies inhibited sporozoite motility and cell invasion. These results suggest that *L. lactis*-produced PfCSP4/38 has the characteristics to be a useful tool for preclinical investigations of *P. falciparum* malaria vaccines.

Experimental procedures

Preparation of construct

Codon-optimized $PfCSP_{26-383}$ containing 4 NDVP and 38 NANP repeats (NCBI reference sequence XM_001351086.1) 3D7 synthesized by (GeneArt®; Life Technologies, Inc.) and inserted into pSS1 (43) plasmid vector for protein expression in *L. lactis*. The final construct, containing a His_6 tag separated by three amino acids (GGS) at its C terminus and denoted PfCSP4/38, was verified by sequencing and transformed into *L. lactis* MG1363 by electroporation as described (44).

Screening, fermentation, and protein purification, 1-liter scale

Screening for expression of PfCSP4/38 protein in *L. lactis* MG1363 was done as described previously (16). Briefly, *L. lactis* MG1363/PfCSP4/38 construct was grown overnight at 30 °C in 5 ml of LAB medium supplemented with 4% glycerol-phosphate, 5% glucose, and 1 μg/ml erythromycin. Culture supernatants were clarified by centrifugation at 9,000 × *g* for 30 min at 4 °C and analyzed by Coomassie-stained SDS-PAGE gel and Western blotting. Fermentation of *L. lactis* MG1363/PfCSP4/38 was performed in a 1-liter lab scale bioreactor (BIOFLO 310; New Brunswick Scientific) at 30 °C with gentle stirring (150 rpm) overnight with pH maintained at 6.5 ± 0.2. Cell-free culture filtrates were concentrated 10-fold and buffer-exchanged into HEPES buffer, pH 7.0 (20 mM HEPES, 50 mM NaCl, 10 mM imidazole) using a QuixStand benchtop system (hollow fiber cartridge with cutoff at 30,000 Da; surface area, 650 cm^2; GE Healthcare). Buffer-exchanged material was applied to a 5-ml Ni^{+2}–nitrilotriacetic acid column (HisTrap HP; GE Healthcare). Bound protein was eluted via step gradient with 700 mM imidazole in HEPES buffer, pH 7.0 (20 mM HEPES, 50 mM NaCl) at a flow rate of 4 ml/min. Eluent fractions were analyzed for purity by SDS-PAGE, pooled, and further applied to a 5-ml cation exchange column (HiTrap SP HP column; GE Healthcare) for polishing and removing host cell protein. Bound protein from the IEC column was eluted through step-gradient elution in HEPES buffer, pH 7.0 (20 mM HEPES, 1 M NaCl, and 1 mM EDTA), and fractions containing pure PfCSP4/38 were concentrated by a VIVA spin column 10-kDa cutoff (Sartorius) in 20 mM HEPES, 200 mM NaCl, and 1 mM EDTA, pH 7.0, and frozen at −80 °C. Fractions were pooled based on SDS-PAGE and immune blotting analysis with 1A6, 1E8, and anti-*L. lactis* antibody. Protein concentration was measured by the BCA protein assay (Thermo Fisher Scientific), and endotoxin content was quantified by Pierce Limulus amebocyte lysate (LAL) chromogenic endotoxin quantitation kit (Thermo Fisher Scientific).

Fermentation and protein purification, 5-liter scale

The process for expression of PfCSP4/38 in *L. lactis* at the 5-liter scale was conducted as previously described with minor modifications. Briefly, fermentation of *L. lactis* MG1363/CSP4/38 was performed in a 5-liter lab-scale bioreactor (BIOFLO 310; New Brunswick Scientific). Buffer-exchanged material was applied to a 20-ml HisPrep FF 16/10 column (GE Healthcare). Bound protein was eluted as previously, and fractions containing the desired protein were applied to a 20-ml HiPrep SP HP 16/10 column (GE Healthcare), where it was eluted through step gradient and concentrated as previous.

SDS-PAGE and immune blotting

Samples were diluted with 6× SDS (SDS, Sigma–Aldrich) sample buffer, heated for 8 min at 98 °C, and loaded in a final volume of 20 μl/well on SDS-PAGE gels (4–12% NuPAGE Bis-Tris, Invitrogen). The gels were run at 150–200 V for 50 min in 1× MOPS SDS running buffer and stained with either Coomassie or InstantBlue protein stain (Expedeon). Following SDS-PAGE, the proteins were transferred onto a nitrocellulose membrane for Western blotting with anti-His-HRP antibody (Miltenyi Biotech), or monoclonal antibodies 1A6 and 1E8. The conformational (1A6) and nonconformational (1E8) monoclonal antibodies were raised from immunization with a full-length PfCSP manufactured by Gennova Biopharmaceuticals (Pune, India) as previously described (45, 46) and kindly provided for this study by PATH. The membranes were blocked in 1% skim milk in TBS containing 0.05% Tween 20 (TBST) at room temperature for 1 h. Primary antibody at a 1 μg/ml of mAb 1A6 or 1E8 (2.0 mg/ml) in TBST was added and incubated for 1 h at room temperature. The membranes were washed with TBST (three times for 5 min) and secondary antibody, and 1:4,000 dilution of goat anti-mouse IgG-HRP conjugated (DAKO, Denmark) in TBST was incubated at room temperature for 1 h. The membranes were again washed with TBST (three times for 5 min), developed using HRP kit (SERA CARE).

Free cysteine detection

The amount of free cysteine residues was measured using Ellman's reagent (Thermo Fisher Scientific) following the manufacturer's instructions. A standard curve was constructed using known concentrations of free cysteine (Sigma–Aldrich).

Analytical size exclusion high-performance liquid SEC-MALS

SEC-MALS experiments were performed on a Dionex (Thermo Scientific) HPLC system connected in-line with a UV detector (Thermo Scientific Dionex™ Ultimate 3000, MWD-

3000), a DAWN HELEOS 8+ multiangle laser light scattering detector, and a Optilab T-rEX (Wyatt Technology Corporation) refractive index detector. SEC was performed on a Superdex 200 Increase 10/300 GL column (GE Healthcare, Sweden) at room temperature in 20 mM Tris, pH 7.5, 200 mM NaCl. 100 μl of PfCSP4/38 were injected at a concentration of 0.9 mg ml^{-1}, and the flow rate was set to 0.5 ml min-1. The ASTRA (version 6.1.17) software (Wyatt Technology Corporation) was used to collect the data from the UV, refractive index, and light scattering detectors. The weight average molecular mass was determined across the elution profile from static light scattering measurements using ASTRA software and a Zimm model that relates the amount of scattered light to the weight average molecular mass of the solute, the concentration of the sample, and the square of the refractive index increment (*dn*/*dc*) of the sample.

RP-HPLC analysis

RP-HPLC was performed using an Agilent 1100 series HPLC system (Agilent Technologies) equipped with equipped with an Agilent Poroshell 300SB-C3 column, 5 μm 2.1 $\times$ 75 mm (Agilent Technologies). 210 pmol of protein (nonreduced) was injected and eluted with a linear gradient of 3–95% over 30 min of 0.1% TFA, 20% isopropanol, and 70% acetonitrile. The absorbance was measured at 215 nm, and chromatographic peaks were integrated by HPLC ChemStation (Agilent Technologies).

Dynamic light scattering

DLS experiments were performed on a DynaPro NanoStar cuvette-based instrument (Wyatt Technology Corporation) operated with Dynamics software (version 7.8.1.3). The data were collected at 20, 25, and 37 °C using a 0.9 mg ml^{-1} PfCSP4/38 sample in 20 mM HEPES, pH 7.0, 200 mM NaCl, 1 mM EDTA. A total of 10 measurements were performed at each temperature. The acquisition time was 5 s, and the read interval was 1 s.

Differential scanning fluorimetry (nano-DSF)

Thermal stability of PfCSP4/38 was measured by label-free nano-DSF using a Prometheus NT.48 instrument (NanoTemper Technologies, Munich, Germany). PfCSP4/38 at a final concentration of 4 μM in 20 mM HEPES, pH 7.0, 200 mM NaCl, 1 mM EDTA was loaded in standard grade capillaries and analyzed over a temperature range from 20C to 90 °C using a heating rate of 1 °C/min. The data were recorded and analyzed with the Prometheus PR.Control (version 1.11) software (NanoTemper Technologies).

Circular dichroism

CD experiments were performed on a Jasco J-815 spectropolarimeter attached to a Peltier temperature control unit PTC-423S thermostat. Samples at 0.15 mg ml^{-1} in 20 mM sodium phosphate, pH 7.2, 50 mM NaF were measured in a 1-mm quartz cuvette. Nine CD spectra were accumulated at 20 or 90 °C in the wavelength range of 190–260 nm with 1-nm bandwidth, response time of 1 s, and scanning speed of 100 nm min^{-1}. The CD data are represented in terms of mean residue ellipticity (deg cm^2 dmol^{-1}).

Mass spectrometry

Accurate molecular mass of full-length PfCSP4/38 was measured by LC–electrospray ionization–MS under both nonreducing and reducing conditions. Approximately 20 pmol of purified protein samples (for the reducing experiments, samples were incubated at room temperature for 30 min with a 10-fold excess of TCEP 0.5 M) were injected into a UPLC system (UltiMate 3000; Dionex) on a MAbPac^{TM} reversed-phase column (Thermo Scientific; 2.1 $\times$ 100 mm, 4-μm particle size) and analyzed with a microOTOF-Q mass spectrometer (Bruker Daltonik GmhH) equipped with an electrospray ionization source (capillary voltage, 4500 V; end plate offset, −500 V; nebulizer gas (nitrogen) pressure, 1.4 bar; flow, 9 ml/min; and drying gas temperature, 190 °C). The LC method uses a gradient of A (98% water, 2% acetonitrile, 0.1% formic acid) and B (98% acetonitrile, 2% water, 0.1% formic acid) with a flow rate of 0.2 ml/min as follows: 0–2 min 5% B, 2–5 min 80% B, 5–7.5 min 80% B, 7.5–9.5 min 5% B, 9.5–12 min 5% B. Data acquisition was done under the control of the module Hystar 3.2-SR 2 from Bruker Compass 1.3 software that integrates both the LC chromatographic separation and MS methods. Data analysis was done with DataAnalysis version 4.0 SP5 (Bruker Daltonik GmhH), with which charge deconvolution was performed using the maximum entropy deconvolution algorithm.

Stability studies

The samples were taken out from −80 °C and incubated for 0, 1, 2, 7, 15, and 30 days at 4 and 37 °C. The samples were analyzed together after end of the 30-day incubation. Additionally, a freeze/thaw stability study was conducted, where the protein was subjected (after initial freeze at production) to additional freeze/thaw of three and five cycles. Samples were analyzed together at the end of the study alongside a control (no additional freeze/thaw cycle). For both studies, SDS-PAGE and Western blots were conducted for samples indicated according to the methods described previously.

Animals and immunogenicity studies

Two *in vivo* animal studies were conducted in mice. For the first study, female 6–8-week-old CD-1 mice (Taconic, Denmark) were kept in the Laboratory Animal Facility Center at Panum, University of Copenhagen, Denmark for 7 days before the first immunization. All procedures regarding animal immunizations complied with European and national regulations. Groups of eight mice were immunized by the subcutaneous route three times at 3-week intervals with 10 μg of PfCSP4/38 absorbed to Alhydrogel®. Vaccine formulations were made immediately prior to use. Responses were measured using sera taken 2 weeks after the third immunization (day 56). The second study was conducted in a similar model as described, but with 20 μg of PfCSP4/38 emulsified in Montanide ISA720VG (Seppic) immediately before use. Immunizations for this second study consisted of a total of two immunizations on days 0 and 28, with terminal sera taken on day 42 for analysis.

Antibody measurements

Levels of plasma antibodies to PfCSP4/38 and GLURP-R2 were measured by ELISA as previously described (16, 47).

Briefly, microtiter plates were coated with 0.33 μg/ml of recombinant protein and incubated with diluted samples (1:200). Bound antibody was detected with HRP-conjugated goat anti-mice IgG-HRP (DAKO).

Sporozoite ELISA

96-well plates were coated with protein lysate from NF54 sporozoites (1,000 sporozoites per well) dissected from salivary glands. After blocking, 11 dilutions (1/10–1/1,000,000) of polyclonal PfCSP4/38 antibodies in 10% mouse sera were added for a total volume of 100 μl/well. Bound PfCSP4/38 antibodies were detected using a horseradish peroxidase–conjugated anti-mouse secondary antibody and quantified using 3,3′,5,5′-tetramethylbenzidin substrate. The color reaction was stopped by adding 100 μl of 0.5 M H_2SO_4. To estimate a corrected concentration of PfCSP-specific antibodies in the mouse sera, each ELISA plate also contained a 5-fold serial dilution (starting from 200 μg/ml) of purified IgG antibody (mAb2A10) to the PfCSP repeat region, used to generate a standard reference curve. The corrected concentration of PfCSP-specific antibodies based on the reference curve was calculated from the ELISA optical density readout using a four-parameter logistic curve fit program (31).

In vitro sporozoite gliding motility assay

Flat-bottomed optical-bottom 96-well plates with a coverglass base were incubated overnight at 4 °C with an anti-PfCSP mAb (3SP2, obtained from Radboud University Medical Center, Nijmegen, The Netherlands). During blocking, five dilutions of 2A10 or polyclonal mouse sera (containing PfCSP4/38 antibodies) were preincubated with sporozoites and thereafter transferred in duplicate onto the plate. Following a 10-min spin at 3,000 rpm, the sporozoites were incubated for 90 min at 37 °C/5% CO_2 on the plate, and thereafter gliding motility was measured as previously described (35). The ;Results were plotted in GraphPad Prism version 5.03. The number of pixels present on a stitched image made from 25 individual pictures taken per well is a measure of the amount of shed PfCSP4/38 in that particular well, and therefore, differences in the number of pixels can be interpreted as differences in sporozoite gliding trail surface (48).

In vitro sporozoite traversal and infectivity assay of a human hepatoma cell line

The HC-04 human hepatoma cell line (42, 49) was acquired through MR4 as part of the Biodefense and Emerging Infections Research Resources Repository (BEI Resources) and cultured as previously described (35). Traversal was conducted as previously described (42, 50) using freshly dissected *P. falciparum* NF54 sporozoites. Briefly, sporozoites were preincubated for 30 min with the monoclonal 2A10 or mouse polyclonal sera containing PfCSP4/38 antibodies. Sporozoite/antibody samples were added in duplicate to HC-04 cells seeded on 384-well plates, along with tetramethylrhodamine (Rh)–labeled dextran (10,000 sporozoites and 12,500 HC-04 cells/well). Sporozoites were allowed to traverse HC-04 cells for 2 h at 37 °C in 5% CO_2 and were then washed in PBS. The level of fluorescence was measured in a Biotek Synergy 2. Data analysis was performed in GraphPad version 5.03. Traversal inhibition was normalized against the assay controls, and the IC_{50} value was calculated by logistic regression using a four-parameter model and the least-square method to determine the best fit.

In vitro primary human hepatocyte invasion and maturation was performed as described in Ref. 44, with a few adaptations. Cryopreserved primary human hepatocytes were obtained from Tebu-bio (donor HC10–10), and they were thawed and seeded at a density of 50,000 cells/well in a collagen-coated 96-well clear-bottomed black plate for 2 days. Per well, 50,000 freshly dissected *Pf*NF54 sporozoites were mixed with monoclonal 2A10 or mouse polyclonal sera containing PfCSP4/38 antibodies for 30 min, after which the mixtures were transferred onto the hepatocytes. After a quick spin (10 min at 1,900 × *g*), the plate was transferred to 37 °C in 5% CO_2. Three hours post-invasion, the medium was refreshed with normal hepatocyte culture medium. The samples were tested in duplicate with daily hepatocyte culture medium refreshments. Four days after sporozoite invasion, hepatocytes were fixed with 4% (v/v) paraformaldehyde. The wells were stained with rabbit anti-*Pf*HSP70, followed by Alexa Fluor 594–labeled goat anti-rabbit IgG and 4′,6-diamidino-2-phenylindole. By using automated high content imaging on a Cytation (BioTek) and FIJI imaging software, both the total number of hepatocytes and the number of positively stained (infected) hepatocytes were determined. Data analysis was performed in GraphPad version 5.03. Invasion inhibition was normalized against the assay controls and the IC_{50} was calculated by logistic regression using a four-parameter model and the least-square method to determine the best fit.

Author contributions—S. K. S., J. P., and M. T. conceptualization; S. K. S., J. P., S. K., E. L., and M. T. resources; S. K. S., B. K. C., V. S., J. M. B., and K. J. D. data curation; S. K. S., J. P., B. K. C., B. A., B. L.-M., and M. T. formal analysis; S. K. S. and M. T. supervision; S. K. S., J. P., V. S., J. M. B., K. J. D., B. A., B. L.-M., S. K., and C. R. K. validation; S. K. S., B. A., and M. T. investigation; S. K. S., J. P., B. K. C., E. L., C. R. K., and M. T. visualization; S. K. S., B. K. C., V. S., J. M. B., K. J. D., and B. L.-M. methodology; S. K. S., J. P., and M. T. writing-original draft; S. K. S., J. P., E. L., and M. T. project administration; J. P., C. R. K., and M. T. writing-review and editing; B. A. and B. L.-M. software.

Acknowledgments—We thank Dr. Sanjay Singh of Gennova Biopharmaceuticals for providing the control E. coli PfCSP protein alongside the monoclonal antibodies 1A6 and 1E8. The proteins and monoclonal antibodies were provided through agreements with PATH and its partners. We thank Tenna Jensen for technical assistance. In addition, the authors thank Ashley Birkett of PATH's Malaria Vaccine Initiative for support and assistance with conceptualization of the work presented here and Scott Gregory of PATH's Malaria Vaccine Initiative for assistance with project support, agreements, technical review of the prepared manuscript, and valuable feedback.

References

1. World Health Organization (2018) *World Malaria Report 2018*, World Health Organization, Geneva, Switzerland
2. Alonso, P. L., Brown, G., Arevalo-Herrera, M., Binka, F., Chitnis, C., Collins, F., Doumbo, O. K., Greenwood, B., Hall, B. F., Levine, M. M., Mendis,

K., Newman, R. D., Plowe, C. V., Rodríguez, M. H., Sinden, R., *et al.* (2011) A research agenda to underpin malaria eradication. *PLoS Med.* **8,** e1000406 CrossRef Medline

3. Cerami, C., Frevert, U., Sinnis, P., Takacs, B., Clavijo, P., Santos, M. J., and Nussenzweig, V. (1992) The basolateral domain of the hepatocyte plasma membrane bears receptors for the circumsporozoite protein of *Plasmodium falciparum* sporozoites. *Cell* **70,** 1021–1033 CrossRef Medline
4. Frevert, U., Sinnis, P., Cerami, C., Shreffler, W., Takacs, B., and Nussenzweig, V. (1993) Malaria circumsporozoite protein binds to heparan sulfate proteoglycans associated with the surface membrane of hepatocytes. *J. Exp. Med.* **177,** 1287–1298 CrossRef Medline
5. Ménard, R., Sultan, A. A., Cortes, C., Altszuler, R., van Dijk, M. R., Janse, C. J., Waters, A. P., Nussenzweig, R. S., and Nussenzweig, V. (1997) Circumsporozoite protein is required for development of malaria sporozoites in mosquitoes. *Nature* **385,** 336–340 CrossRef Medline
6. Gordon, D. M., McGovern, T. W., Krzych, U., Cohen, J. C., Schneider, I., LaChance, R., Heppner, D. G., Yuan, G., Hollingdale, M., and Slaoui, M. (1995) Safety, immunogenicity, and efficacy of a recombinantly produced *Plasmodium falciparum* circumsporozoite protein-hepatitis B surface antigen subunit vaccine. *J. Infect. Dis.* **171,** 1576–1585 CrossRef Medline
7. Agnandji, S. T., Lell, B., Fernandes, J. F., Abossolo, B. P., Methogo, B. G., Kabwende, A. L., Adegnika, A. A., Mordmuller, B., Issifou, S., Kremsner, P. G., Sacarlal, J., Aide, P., Lanaspa, M., Aponte, J. J., Machevo, S., *et al.* (2012) A phase 3 trial of RTS,S/AS01 malaria vaccine in African infants. *N. Engl. J. Med.* **367,** 2284–2295 CrossRef Medline
8. Agnandji, S. T., Lell, B., Soulanoudjingar, S. S., Fernandes, J. F., Abossolo, B. P., Conzelmann, C., Methogo, B. G., Doucka, Y., Flamen, A., Mordmüller, B., Issifou, S., Kremsner, P. G., Sacarlal, J., Aide, P., Lanaspa, M., *et al.* (2011) First results of phase 3 trial of RTS,S/AS01 malaria vaccine in African children. *N. Engl. J. Med.* **365,** 1863–1875 CrossRef Medline
9. Gosling, R., and von Seidlein, L. (2016) The future of the RTS,S/AS01 malaria vaccine: an alternative development plan. *PLoS Med.* **13,** e1001994 CrossRef Medline
10. Young, J. F., Hockmeyer, W. T., Gross, M., Ballou, W. R., Wirtz, R. A., Trosper, J. H., Beaudoin, R. L., Hollingdale, M. R., Miller, L. H., and Diggs, C. L. (1985) Expression of *Plasmodium falciparum* circumsporozoite proteins in *Escherichia coli* for potential use in a human malaria vaccine. *Science* **228,** 958–962 CrossRef Medline
11. Noe, A. R., Espinosa, D., Li, X., Coelho-Dos-Reis, J. G., Funakoshi, R., Giardina, S., Jin, H., Retallack, D. M., Haverstock, R., Allen, J. R., Vedvick, T. S., Fox, C. B., Reed, S. G., Ayala, R., Roberts, B., Winram, S. B., *et al.* (2014) A full-length *Plasmodium falciparum* recombinant circumsporozoite protein expressed by *Pseudomonas fluorescens* platform as a malaria vaccine candidate. *PLoS One* **9,** e107764 CrossRef Medline
12. Schwenk, R., DeBot, M., Porter, M., Nikki, J., Rein, L., Spaccapelo, R., Crisanti, A., Wightman, P. D., Ockenhouse, C. F., and Dutta, S. (2014) IgG2 antibodies against a clinical grade *Plasmodium falciparum* CSP vaccine antigen associate with protection against transgenic sporozoite challenge in mice. *PLoS One* **9,** e111020 CrossRef Medline
13. Kedees, M. H., Azzouz, N., Gerold, P., Shams-Eldin, H., Iqbal, J., Eckert, V., and Schwarz, R. T. (2002) *Plasmodium falciparum*: glycosylation status of *Plasmodium falciparum* circumsporozoite protein expressed in the baculovirus system. *Exp. Parasitol.* **101,** 64–68 CrossRef Medline
14. Plassmeyer, M. L., Reiter, K., Shimp, R. L., Jr., Kotova, S., Smith, P. D., Hurt, D. E., House, B., Zou, X., Zhang, Y., Hickman, M., Uchime, O., Herrera, R., Nguyen, V., Glen, J., Lebowitz, J., *et al.* (2009) Structure of the *Plasmodium falciparum* circumsporozoite protein, a leading malaria vaccine candidate. *J. Biol. Chem.* **284,** 26951–26963 CrossRef Medline
15. Singh, S. K., Tiendrebeogo, R. W., Chourasia, B. K., Kana, I. H., Singh, S., and Theisen, M. (2018) *Lactococcus lactis* provides an efficient platform for production of disulfide-rich recombinant proteins from *Plasmodium falciparum*. *Microbial Cell Factories* **17,** 55 CrossRef Medline
16. Singh, S. K., Roeffen, W., Mistarz, U. H., Chourasia, B. K., Yang, F., Rand, K. D., Sauerwein, R. W., and Theisen, M. (2017) Construct design, production, and characterization of *Plasmodium falciparum* 48/45 R0.6C subunit protein produced in *Lactococcus lactis* as candidate vaccine. *Microbial Cell Factories* **16,** 97 CrossRef Medline
17. Theisen, M., Roeffen, W., Singh, S. K., Andersen, G., Amoah, L., van de Vegte-Bolmer, M., Arens, T., Tiendrebeogo, R. W., Jones, S., Bousema, T., Adu, B., Dziegiel, M. H., Christiansen, M., and Sauerwein, R. (2014) A multi-stage malaria vaccine candidate targeting both transmission and asexual parasite life-cycle stages. *Vaccine* **32,** 2623–2630 CrossRef Medline
18. Zhao, J., Bhanot, P., Hu, J., and Wang, Q. (2016) A comprehensive analysis of Plasmodium circumsporozoite protein binding to hepatocytes. *PLoS One* **11,** e0161607 CrossRef Medline
19. Oyen, D., Torres, J. L., Wille-Reece, U., Ockenhouse, C. F., Emerling, D., Glanville, J., Volkmuth, W., Flores-Garcia, Y., Zavala, F., Ward, A. B., King, C. R., and Wilson, I. A. (2017) Structural basis for antibody recognition of the NANP repeats in *Plasmodium falciparum* circumsporozoite protein. *Proc. Natl. Acad. Sci. U.S.A.* **114,** E10438–E10445 CrossRef Medline
20. Oyen, D., Torres, J. L., Wille-Reece, U., Ockenhouse, C. F., Emerling, D., Glanville, J., Volkmuth, W., Flores-Garcia, Y., Zavala, F., Ward, A. B., King, C. R., and Wilson, I. A. (2017) Structural basis for antibody recognition of the NANP repeats in *Plasmodium falciparum* circumsporozoite protein. *Proc. Natl. Acad. Sci. U.S.A.* **114,** E10438–E10445 CrossRef Medline
21. Rathore, D., Nagarkatti, R., Jani, D., Chattopadhyay, R., de la Vega, P., Kumar, S., and McCutchan, T. F. (2005) An immunologically cryptic epitope of *Plasmodium falciparum* circumsporozoite protein facilitates liver cell recognition and induces protective antibodies that block liver cell invasion. *J. Biol. Chem.* **280,** 20524–20529 CrossRef Medline
22. Tan, J., Sack, B. K., Oyen, D., Zenklusen, I., Piccoli, L., Barbieri, S., Foglierini, M., Fregni, C. S., Marcandalli, J., Jongo, S., Abdulla, S., Perez, L., Corradin, G., Varani, L., Sallusto, F., *et al.* (2018) A public antibody lineage that potently inhibits malaria infection through dual binding to the circumsporozoite protein. *Nat. Med.* **24,** 401–407 CrossRef Medline
23. Kisalu, N. K., Idris, A. H., Weidle, C., Flores-Garcia, Y., Flynn, B. J., Sack, B. K., Murphy, S., Schön, A., Freire, E., Francica, J. R., Miller, A. B., Gregory, J., March, S., Liao, H. X., Haynes, B. F., *et al.* (2018) A human monoclonal antibody prevents malaria infection by targeting a new site of vulnerability on the parasite. *Nat. Med.* **24,** 408–416 CrossRef Medline
24. Nussenzweig, R. S., and Nussenzweig, V. (1989) Antisporozoite vaccine for malaria: experimental basis and current status. *Rev. Infect. Dis.* **11,** S579–S585 CrossRef Medline
25. Foquet, L., Hermsen, C. C., van Gemert, G. J., Van Braeckel, E., Weening, K. E., Sauerwein, R., Meuleman, P., and Leroux-Roels, G. (2014) Vaccine-induced monoclonal antibodies targeting circumsporozoite protein prevent *Plasmodium falciparum* infection. *J. Clin. Invest.* **124,** 140–144 CrossRef Medline
26. Romero, P., Maryanski, J. L., Corradin, G., Nussenzweig, R. S., Nussenzweig, V., and Zavala, F. (1989) Cloned cytotoxic T cells recognize an epitope in the circumsporozoite protein and protect against malaria. *Nature* **341,** 323–326 CrossRef Medline
27. Overstreet, M. G., Cockburn, I. A., Chen, Y. C., and Zavala, F. (2008) Protective CD8 T cells against *Plasmodium* liver stages: immunobiology of an "unnatural" immune response. *Immunol. Rev.* **225,** 272–283 CrossRef Medline
28. Collins, K. A., Snaith, R., Cottingham, M. G., Gilbert, S. C., and Hill, A. V. S. (2017) Enhancing protective immunity to malaria with a highly immunogenic virus-like particle vaccine. *Sci. Rep.* **7,** 46621–46621 CrossRef Medline
29. Whitmore, L., and Wallace, B. A. (2004) DICHROWEB, an online server for protein secondary structure analyses from circular dichroism spectroscopic data. *Nucleic Acids Res.* **32,** W668–W673 CrossRef Medline
30. Compton, L. A., and Johnson, W. C., Jr. (1986) Analysis of protein circular dichroism spectra for secondary structure using a simple matrix multiplication. *Anal. Biochem.* **155,** 155–167 CrossRef Medline
31. Adu, B., Cherif, M. K., Bosomprah, S., Diarra, A., Arthur, F. K., Dickson, E. K., Corradin, G., Cavanagh, D. R., Theisen, M., Sirima, S. B., Nebie, I., and Dodoo, D. (2016) Antibody levels against GLURP R2, MSP1 block 2 hybrid and AS202.11 and the risk of malaria in children living in hyperendemic (Burkina Faso) and hypo-endemic (Ghana) areas. *Malar. J.* **15,** 123 CrossRef Medline

32. Theisen, M., Adu, B., Mordmüller, B., and Singh, S. (2017) The GMZ2 malaria vaccine: from concept to efficacy in humans. *Expert Rev. Vaccines* **16,** 907–917 CrossRef Medline
33. do Rosario, V. E., Appiah, A., Vaughan, J. A., and Hollingdale, M. R. (1989) *Plasmodium falciparum*: administration of anti-sporozoite antibodies during sporogony results in production of sporozoites which are not neutralized by human anti-circumsporozoite protein vaccine sera. *Trans. R. Soc. Trop. Med. Hyg.* **83,** 305–307 CrossRef Medline
34. Stewart, M. J., Nawrot, R. J., Schulman, S., and Vanderberg, J. P. (1986) *Plasmodium berghei* sporozoite invasion is blocked *in vitro* by sporozoite-immobilizing antibodies. *Infect. Immun.* **51,** 859–864 Medline
35. Barry, A., Behet, M. C., Nébié, I., Lanke, K., Grignard, L., Ouedraogo, A., Soulama, I., Drakeley, C., Sauerwein, R., Bolscher, J. M., Dechering, K. J., Bousema, T., Tiono, A. B., and Gonçalves, B. P. (2018) Functional antibodies against *Plasmodium falciparum* sporozoites are associated with a longer time to qPCR-detected infection among schoolchildren in Burkina Faso. *Wellcome Open Res.* **3,** 159 CrossRef Medline
36. Ishino, T., Yano, K., Chinzei, Y., and Yuda, M. (2004) Cell-passage activity is required for the malarial parasite to cross the liver sinusoidal cell layer. *PLoS Biol.* **2,** E4 CrossRef Medline
37. Herrera, R., Anderson, C., Kumar, K., Molina-Cruz, A., Nguyen, V., Burkhardt, M., Reiter, K., Shimp, R., Jr., Howard, R. F., Srinivasan, P., Nold, M. J., Ragheb, D., Shi, L., DeCotiis, M., Aebig, J., *et al.* (2015) Reversible conformational change in the *Plasmodium falciparum* circumsporozoite protein masks its adhesion domains. *Infect. Immun.* **83,** 3771–3780 CrossRef Medline
38. Doud, M. B., Koksal, A. C., Mi, L. Z., Song, G., Lu, C., and Springer, T. A. (2012) Unexpected fold in the circumsporozoite protein target of malaria vaccines. *Proc. Natl. Acad. Sci. U.S.A.* **109,** 7817–7822 CrossRef Medline
39. Kana, I. H., Adu, B., Tiendrebeogo, R. W., Singh, S. K., Dodoo, D., and Theisen, M. (2017) Naturally acquired antibodies target the glutamate-rich protein on intact merozoites and predict protection against febrile malaria. *J. Infect. Dis.* **215,** 623–630 CrossRef Medline
40. Hollingdale, M. R., Nardin, E. H., Tharavanij, S., Schwartz, A. L., and Nussenzweig, R. S. (1984) Inhibition of entry of *Plasmodium falciparum* and *P. vivax* sporozoites into cultured cells; an *in vitro* assay of protective antibodies. *J. Immunol.* **132,** 909–913 Medline
41. Vanderberg, J. P., and Frevert, U. (2004) Intravital microscopy demonstrating antibody-mediated immobilisation of *Plasmodium berghei* sporozoites injected into skin by mosquitoes. *Int. J. Parasitol* **34,** 991–996 CrossRef Medline
42. Kurtovic, L., Behet, M. C., Feng, G., Reiling, L., Chelimo, K., Dent, A. E., Mueller, I., Kazura, J. W., Sauerwein, R. W., Fowkes, F. J. I., and Beeson, J. G. (2018) Human antibodies activate complement against *Plasmodium falciparum* sporozoites, and are associated with protection against malaria in children. *BMC Med.* **16,** 61 CrossRef Medline
43. Singh, S. K., Roeffen, W., Andersen, G., Bousema, T., Christiansen, M., Sauerwein, R., and Theisen, M. (2015) A *Plasmodium falciparum* 48/45 single epitope R0.6C subunit protein elicits high levels of transmission blocking antibodies. *Vaccine* **33,** 1981–1986 CrossRef Medline
44. Theisen, M., Soe, S., Brunstedt, K., Follmann, F., Bredmose, L., Israelsen, H., Madsen, S. M., and Druilhe, P. (2004) A *Plasmodium falciparum* GLURP-MSP3 chimeric protein: expression in *Lactococcus lactis*, immunogenicity and induction of biologically active antibodies. *Vaccine* **22,** 1188–1198 CrossRef Medline
45. Kastenmüller, K., Espinosa, D. A., Trager, L., Stoyanov, C., Salazar, A. M., Pokalwar, S., Singh, S., Dutta, S., Ockenhouse, C. F., Zavala, F., and Seder, R. A. (2013) Full-length *Plasmodium falciparum* circumsporozoite protein administered with long-chain poly(I·C) or the Toll-like receptor 4 agonist glucopyranosyl lipid adjuvant-stable emulsion elicits potent antibody and CD4+ T cell immunity and protection in mice. *Infect. Immun.* **81,** 789–800 CrossRef Medline
46. Espinosa, D. A., Christensen, D., Muñoz, C., Singh, S., Locke, E., Andersen, P., and Zavala, F. (2017) Robust antibody and $CD8^+$ T-cell responses induced by *P. falciparum* CSP adsorbed to cationic liposomal adjuvant CAF09 confer sterilizing immunity against experimental rodent malaria infection. *NPJ Vaccines* **2,** 10 CrossRef Medline
47. Lousada-Dietrich, S., Jogdand, P. S., Jepsen, S., Pinto, V. V., Ditlev, S. B., Christiansen, M., Larsen, S. O., Fox, C. B., Raman, V. S., Howard, R. F., Vedvick, T. S., Ireton, G., Carter, D., Reed, S. G., and Theisen, M. (2011) A synthetic TLR4 agonist formulated in an emulsion enhances humoral and type 1 cellular immune responses against GMZ2: a GLURP-MSP3 fusion protein malaria vaccine candidate. *Vaccine* **29,** 3284–3292 CrossRef Medline
48. Boes, A., Spiegel, H., Kastilan, R., Bethke, S., Voepel, N., Chudobová, I., Bolscher, J. M., Dechering, K. J., Fendel, R., Buyel, J. F., Reimann, A., Schillberg, S., and Fischer, R. (2016) Analysis of the dose-dependent stage-specific *in vitro* efficacy of a multi-stage malaria vaccine candidate cocktail. *Malar. J.* **15,** 279 CrossRef Medline
49. Sattabongkot, J., Yimamnuaychoke, N., Leelaudomlipi, S., Rasameesoraj, M., Jenwithisuk, R., Coleman, R. E., Udomsangpetch, R., Cui, L., and Brewer, T. G. (2006) Establishment of a human hepatocyte line that supports *in vitro* development of the exo-erythrocytic stages of the malaria parasites *Plasmodium falciparum* and *P. vivax*. *Am. J. Trop. Med. Hyg.* **74,** 708–715 CrossRef Medline
50. Behet, M. C., Kurtovic, L., van Gemert, G. J., Haukes, C. M., Siebelink-Stoter, R., Graumans, W., van de Vegte-Bolmer, M. G., Scholzen, A., Langereis, J. D., Diavatopoulos, D. A., Beeson, J. G., and Sauerwein, R. W. (2018) The complement system contributes to functional antibody-mediated responses induced by immunization with *Plasmodium falciparum* malaria sporozoites. *Infect. Immun.* **86,** e00920-17 Medline